



Dynamic scaling behavior of human brain electroencephalogram

J.W. Yuan^a, B. Zheng^{a,b,*}, C.P. Pan^c, Y.Z. Wu^a, S. Trimper^b

^aZhejiang University, Zhejiang Institute of Modern Physics, Hangzhou 310027, PR China

^bFB Physik, Universität-Halle, 06099 Halle, Germany

^cCenter for Experimental BioInformatics, University of Southern Denmark, Campusvej 55, DK-5230 Odense M, Denmark

Abstract

After filtering out the α and β peaks in the power spectrum of the human brain electroencephalogram signals $Y(t')$, the probability distribution of the variation $\Delta Y(t') \equiv Y(t' + \Delta t) - Y(t')$ exhibits a dynamic scaling behavior. The auto-correlation functions, persistence probabilities and detrended fluctuation functions of the time series $|\Delta Y(t')|$ all show a nontrivial power-law behavior. These results indicate that the dynamics of the human brain electroencephalogram is long-range correlated in time.

© 2005 Published by Elsevier B.V.

Keywords: Dynamic scaling behavior; Time series; Electroencephalogram

1. Introduction

In recent years, it was suggested that the universal scaling behavior exists in a variety of many-body systems in nature, which may not necessarily exhibit explicit phase transitions [1,2]. Along this understanding, many activities in the past years have been devoted to the application of physical concepts and methods to complex biological, meteorological and economic systems [3–12]. Due to interactions among elements in the complex systems, *long-range* spatial and/or temporal correlations are often generated. These systems are then referred to be scale-free. A characteristic of the scale-free systems is the scaling behavior.

An example of complex biological systems is the heartbeat. With the detrended fluctuation analysis (DFA), the time series of the heartbeat has been analyzed [4,13]. By decomposing the time series $dY(t')$ into two series' $|dY(t')|$ and $\text{sgn}(dY(t'))$, one finds that $|dY(t')|$ is long-range correlated in time, while $dY(t')$ and $\text{sgn}(dY(t'))$ are temporally anti-correlated. The analysis offers some insight into the heartbeat, and reveals a different scaling behavior for heart failure patients. Therefore, the scaling behavior is interesting not only in physical sense. It provides an intrinsic description of the systems, and may also find applications or potential applications [4,5,13,14].

*Corresponding author. Zhejiang University, Zhejiang Institute of Modern Physics, Hangzhou 310027, PR China.

E-mail addresses: bozheng@zju.edu.cn, zheng@zimp.zju.edu.cn (B. Zheng).

The human brain electroencephalogram (EEG) is another very important complex biological system, and has attracted much attention of physicists and scientists in different areas. Different methods, such as the nonlinear dynamic approach, coherence analysis, synchronization study, statistical and various quantitative methods, have been developed for the study of the EEG. From the view of statistical physics, the time series of the human brain EEG is not scale-free in the rigorous sense, since the α and β peaks in the power spectrum just represent some typical time scales. The authors of Refs. [3,15] concentrate the attention on the α and β peaks in the o and p channels, and discover that the *amplitude* of the oscillations is long-range correlated in time. The auto-correlation function of the amplitude is calculated, and the DFA analysis is also used for demonstrating the long-range temporal correlation.

Even though the α and β peaks are the features of the human brain EEG, one may expect that not all the information is contained in these specific oscillations. Therefore, it is interesting and important to study the general time series of the human brain EEG. In a very recent work [16], a first approach based on the DFA method has been presented for the human brain EEG with *closed eyes*. Within the framework of the DFA analysis, the α oscillation appears to be a perturbation only. From the scaling exponent, it is suggested that the time series $|dY(t')|$ is long-range correlated in time, while $dY(t')$ is anti-correlated, at least in the time regime, we investigate. This is similar to the case of the heartbeat. In addition, certain effects of the AD disease are also observed.

The purpose of this article is to reveal more explicitly the long-range temporal correlation, and especially the dynamic scaling behavior of the human brain EEG. We also extend the analysis to the experimental data with both closed and open eyes. In Section 2, a filtering technique is introduced through the Fourier transformation, to study the effect of α and β oscillations. Then, the dynamic scaling behavior of $\Delta Y(t')$ is investigated. In Section 3, we calculate the auto-correlation functions and persistence probabilities to directly uncover the long-range temporal correlation of $|\Delta Y(t')|$. In Section 4, the DFA analysis will be presented. Finally, comes the conclusion.

2. Data analysis and probability distribution

Our experimental data are of 20 healthy individuals and 14 AD patients with closed eyes, and of 19 healthy individuals and 20 AD patients with open eyes. $o1$ and $o2$ channels are measured on the occipital region, $p3$ and $p4$ channels on the parietal region, $t3$ and $t4$ channels on the temporal region, $c3$ and $c4$ channels on the central region, and $f3$ and $f4$ channels on the frontal region [16]. Experimental measurements are performed every $\frac{1}{250}$ s, and last for a total time $T = 130$ s. If not specified, the *time unit is taken to be* $\frac{1}{250}$ s in this paper. In addition, we also have a limited amount of experimental data with a total time T longer than 10 min. These data confirm the results with $T = 130$ s.

Let us denote the EEG time series as $Y(t')$. To have a first view of the time series of the EEG, we perform a standard Fourier transformation of $Y(t')$. The power spectrum $P(f)$ of a *single* healthy individual with closed eyes is displayed for the $o1$ and $f3$ channels with solid lines in Fig. 1. We can see a clear α peak.

An observation in Fig. 1 is that the power spectrum $P(f)$ is power-law-like. The α and β peaks look like ‘perturbations’ only. The slopes of the curves are about $3/4$. The curves drop down in high frequency regime, may be because the highest frequency in the experimental measurements is 250 Hz. Therefore, one may expect that the human brain EEG is scale free, but with possible effects of the α and β peaks.

To investigate the effects of the α and β peaks, we introduce a *filtering technique*. We first transform the time series to the Fourier space, and filter out the α peak and possible β peak of the power spectrum $P(f)$ in the Fourier space, and then transform it back to the configuration space. We denote this refined time series as $Y_c(t')$. Since the β peak in the EEG is usually not very prominent [3], this filtering technique mainly concerns the α peak. In Fig. 1, the power spectra of $Y_c(t')$ are also plotted with square lines. For some properties, $Y(t')$ and $Y_c(t')$ yield invisible difference, and the α and β oscillations look indeed like irrelevant perturbations only; For other properties, the effect of the α and β peaks can be clearly observed, and even rather important in understanding the dynamics of the human brain EEG.

Let us consider the variation $\Delta Y(t') \equiv Y(t' + \Delta t) - Y(t')$, keeping in mind that our time unit is $\frac{1}{250}$ s. The probability distribution of $\Delta Y(t')$, denoted as $P(\Delta Y, \Delta t)$, generally depends on Δt . This is shown in Fig. 2(a) for the $o1$ channel of the AD patients with closed eyes before filtering out the α and β peaks. One does not observe any dynamic scaling behavior.

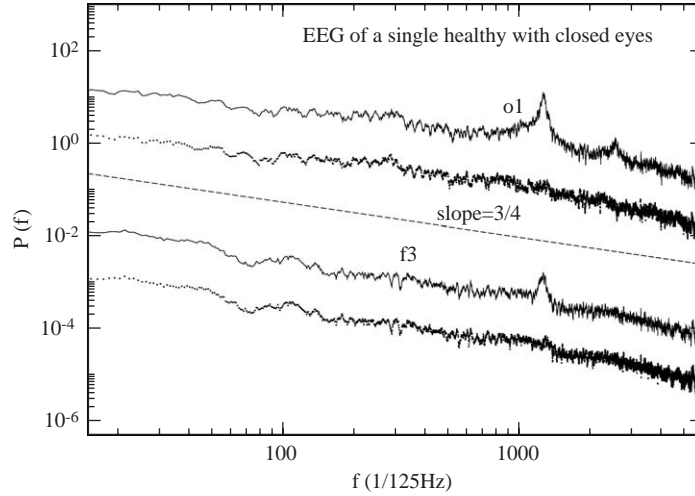


Fig. 1. Power spectra for the $o1$ and $f3$ channels of a single healthy individual with closed eyes are displayed with solid lines in log–log scale. The square lines show those after filtering out the α and β peaks.

We now demonstrate that the probability distribution $P(\Delta Y_c, \Delta t)$ exhibits a dynamic scaling behavior, after filtering out the α and β oscillations. From a general view of statistical physics, one may expect a dynamic scaling form for a scale-free system

$$P(\Delta Y_c, \Delta t) \sim \Delta t^{-1/\alpha} F(\Delta Y_c / \Delta t^{1/\alpha}) \quad (1)$$

with α being an exponent. To reveal the dynamic scaling form in Eq. (1), we perform a scaling plot of the distribution $P(\Delta Y_c, \Delta t)$ with different time Δt . This is shown in Fig. 2(b) for the $o1$ channel of the AD patients with closed eyes. Even though the data are slightly fluctuating, the data collapse is clearly observed. The exponent $1/\alpha$ is estimated to be about 0.16. Similar data collapses are observed for all the healthy individuals and AD patients with both open and closed eyes. Qualitatively, we observe that the exponent $1/\alpha$ of the AD patients is somewhat bigger than that of the healthy individuals, but to clarify this point, we need more careful analysis. The fluctuation in the data collapse is too large for this purpose. Our analysis also yields similar results for both cases with open and closed eyes.

Here a grand average over all individuals has been performed to reduce the fluctuation. Such an average is often reported in literature [3,15]. We believe that if there are sufficient data for a single individual, the grand average is not necessary.

We must emphasize, however, that without filtering out the α and β oscillations, the data do not collapse. One can understand this in Fig. 2(a). The filtering technique here plays an important role in revealing the dynamic scaling behavior of the human brain EEG.

To summarize, the dynamic scaling behavior of $P(\Delta Y_c, \Delta t)$ after filtering out the α and β peaks indicates that the human brain EEG is a quasi-scale-free dynamic system. The exponent $1/\alpha$ of the AD patients seems slightly bigger than that of the healthy individuals.

3. Auto-correlations and persistence probabilities

The analysis of the dynamic scaling behavior in the preceding section suggests that the time series of the human brain EEG may be long-range correlated in time. The auto-correlation function directly measures the time correlation of a time series. As an example, we consider the time series $dY(t) \equiv Y(t+1) - Y(t)$. Since $dY(t)$ is anti-correlated in time, it is illustrating to define the auto-correlation function of $|dY(t)|$

$$A(t) = \langle |dY(t)||dY(t+t)| \rangle - (\langle |dY(t)| \rangle)^2. \quad (2)$$

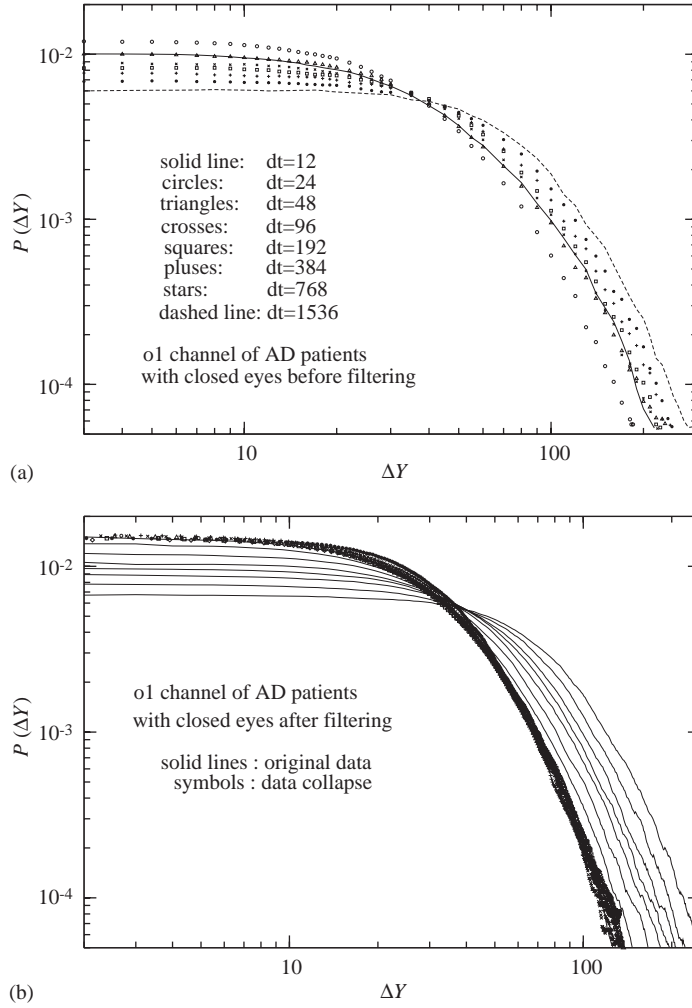


Fig. 2. (a) The probability distribution $P(\Delta Y, \Delta t)$ for the o1 channel of the AD patients with closed eyes before filtering out the α peak, (b) the scaling plot of $P(\Delta Y_c, \Delta t)$ for the o1 channel of the AD patients with closed eyes after filtering out the α peak. Solid line are for $\Delta t = 12, 24, 48, 96, 192, 384, 768, 1536$ (from the left). Symbols fitted to the curve of $\Delta t = 12$ are the data of other Δt 's rescaled suitably according to Eq. (1) with the exponent $1/\alpha = 0.16$.

Here the average $\langle \dots \rangle$ is taken over t' and also different individuals. Typically, the measurement of $A(t)$ may be fluctuating, but $A(t)$ does give a clear evidence whether the time series is correlated in time, at least qualitatively. If the time series is uncorrelated in time or with a short correlating time, $A(t)$ drops to zero exponentially. If the time series is long-range correlated in time, $A(t)$ decays by a power-law.

$$A(t) \sim t^{-\beta}. \quad (3)$$

In Fig. 3(a), the auto-correlation functions of the o1, p3, c3, t3 and f3 channels are displayed for both healthy individuals and AD patients with *open eyes* in log-log scale. In general, the curves of the AD patients exhibit a relatively clean power-law behavior, and the exponent β takes values between 0.5 and 1.0, depending on the channels. The curves of the healthy individuals are somewhat fluctuating, but look still power-law-like.

For all the channels except for t3 and t4 with *open eyes*, the exponent β of the AD patients looks smaller than that of the healthy individuals. Such a result seems understandable. A smaller value of the exponent β indicates a slower dynamics. For AD patients, connections of many neural cells are already weaken or

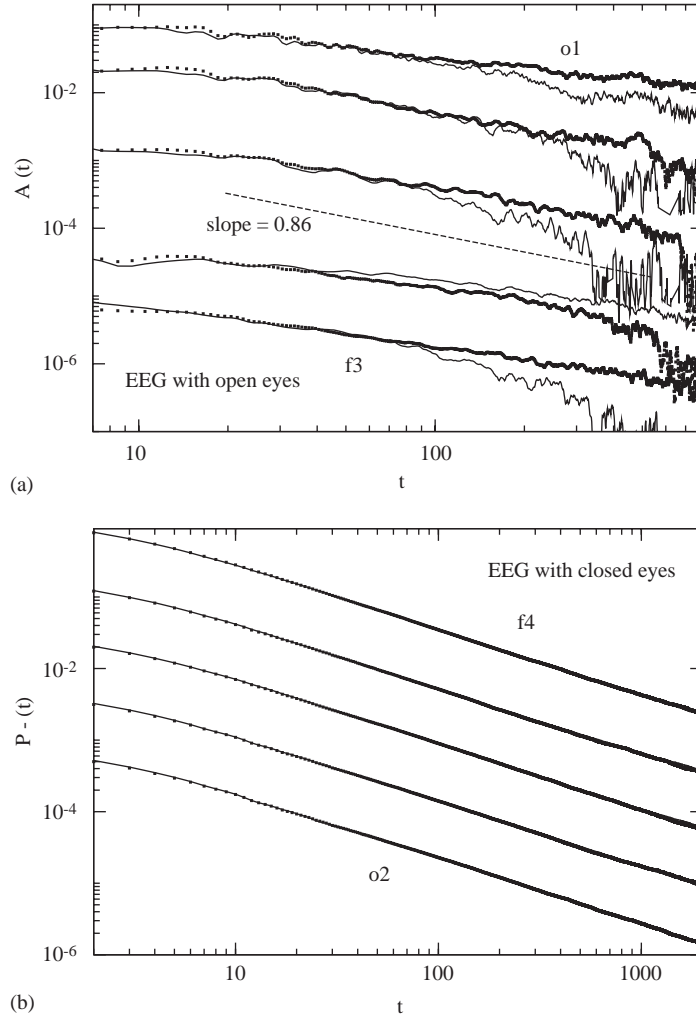


Fig. 3. (a) Auto-correlation functions of $|dY(t')|$ for the $o1$, $p3$, $c3$, $t3$ and $f3$ channels (from above) for both healthy individuals (solid lines) and AD patients (square lines) with open eyes in log–log scale. (b) The persistence probability $P_-(t)$ of the $o2$, $p4$, $c4$, $t4$ and $f4$ channels (from below) with closed eyes. Solid lines and square lines are for healthy individuals and AD patients, respectively. To guide the eyes, curves in the figure have been shifted suitably.

blocked, therefore, the dynamics is slowed down. It is consistent with the earlier finding that the amplitude of low frequencies in the power spectrum of the EEG increases for AD patients [17].

The technique of filtering out the α and β oscillations does not change the results above. Our calculations of the auto-correlation functions directly show that the time series of the human brain EEG is scale-free for both healthy individuals and AD patients, and therefore, a universal dynamic scaling behavior may be expected. This physically explains the dynamic scaling behavior of $P(\Delta Y_c, \Delta t)$ described in the previous section.

A natural question is how the auto-correlation function of the time series of $dY(t')$ behaves. The answer is that $dY(t')$ is anti-correlated in time, and therefore, it is somewhat difficult to measure its auto-correlation function. The DFA analysis in the next section will reveal this phenomenon clearly.

For further understanding the long-range temporal correlation in the EEG dynamics, we now calculate the persistence probability of the time series. The auto-correlation function measures the correlation *local* in time, while the persistence probability detects the correlation *nonlocal* in time. As time evolves, the persistence probability of a critical dynamic system decays by a power law characterized by a persistence exponent θ_p ,

$$P(t) \sim t^{-\theta_p}. \quad (4)$$

It is shown that the persistence exponent is in general *independent* of other known critical exponents [18]. The persistence exponent plays an important role in a variety of systems and has been directly measured in experiments [18–21].

Let us define the persistence probability $P_+(t)$ ($P_-(t)$) as the probability that $|dY(t' + \tilde{t})|$ has always been above (below) $|dY(t')|$ in time t , i.e., $|dY(t' + \tilde{t})| > |dY(t')|$ ($|dY(t' + \tilde{t})| < |dY(t')|$) for all $\tilde{t} < t$. The average is taken over the time variable t' and all the individuals.

For an uncorrelated Gaussian process, both $P_+(t)$ and $P_-(t)$ decay by a power law with an exponent $\theta_p = 1.0$. Therefore, deviation of the exponent θ_p from 1.0 indicates that the dynamic process is long-range correlated in time. In Fig. 3(b), $P_-(t)$ for the EEG with closed eyes are plotted in log–log scale. A nice power-law behavior is observed for both healthy individuals and AD patients, and the fluctuation here is much less than that of the auto-correlation functions. The exponent θ_p takes values between 0.85 and 0.93, which differ from 1.0 by about 10%, and this clearly indicates that the time series of $|dY(t')|$ is long-range correlated in time. But the persistence probability seems not detecting the effect of the AD disease.

In summary, our calculations of the auto-correlation functions and persistence probabilities directly show that the time series of $|dY(t')|$ ($|dY_c(t')|$) is long-range correlated in time. The results seem to indicate that the dynamics of AD patients is slower than that of healthy individuals.

4. DFA analysis

The auto-correlation function is a principal observable for measuring the time correlation, but may require sufficiently more data to achieve a good accuracy. The DFA analysis is a simple but powerful method for revealing the temporal correlation of a time series, and helps remove the trends in the time series. This method was proposed a decade ago [13,22], and has been applied to a variety of physical systems, and shows its efficiency [23,24].

Let us first introduce the DFA method [13,22]. For a fluctuating dynamic series $dB(t')$, we construct an integrated time series

$$C(t') = \sum_{t''=1}^{t'} [dB(t'') - dB_{ave}]. \quad (5)$$

Here dB_{ave} is the average of $dB(t'')$ in the total time interval $[1, T]$. Then, we uniformly divide the interval $[1, T]$ into windows with a size of t , and linearly fit $C(t')$ to a linear function $C_t(t')$ in each window. Finally, we calculate the DFA function

$$F(t) = \sqrt{\frac{1}{T} \sum_{t'=1}^T [C(t') - C_t(t')]^2}. \quad (6)$$

In general, $F(t)$ obeys a power-law behavior

$$F(t) \sim t^\theta. \quad (7)$$

If $0 < \theta < 0.5$, $dB(t')$ is long-range anti-correlated; if $0.5 < \theta < 1.0$, $dB(t')$ is long-range correlated. $\theta = 0.5$ corresponds to the Gaussian white noise, while $\theta = 1.0$ indicates the $1/f$ noise. If the integration procedure in Eq. (5) is performed one more time, the DFA function $F(t) \sim t^{\theta+1}$ [4].

Therefore, the DFA method can be applied to both $dY(t')$ and $Y(t')$ of the EEG, and the DFA function behaves like $F(t) \sim t^\theta$ and $t^{\theta+1}$, respectively. In Fig. 4, the DFA function calculated from $Y(t')$ with closed eyes is displayed on a log–log scale. To obtain the curves, a grand average has been also performed. In the early times, one observes deviation from the power-law behavior. Especially, the weak ‘oscillation’ of the curves around $t = 25$ indicates the perturbation of the α peak, which is more prominent for the o channels and becomes almost invisible for the f channels. After $t \sim 100$, $F(t)$ gradually converges to a power-law behavior. From the figures, one clearly sees that the curves of the AD patients increase faster than those of the healthy individuals.

In the left sector of Table 1, the values of $\theta + 1$ measured from figures like Fig. 4 are given. Errors are those from the grand average, and the fluctuations along the time direction are also taken into account. Both θ_n for

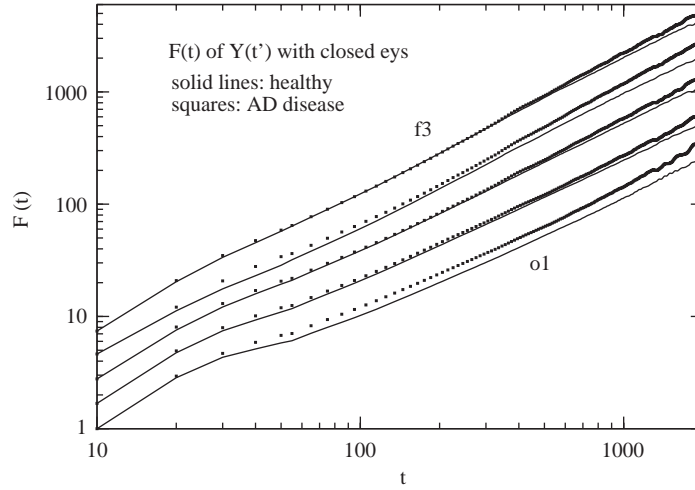


Fig. 4. DFA functions of $Y(t')$ for the EEG with closed eyes in log-log scale. Solid lines and square lines are for healthy individuals and AD patients, respectively. From below, the curves are of the $o1$, $p3$, $c3$, $t3$ and $f3$ channels.

Table 1

In the left sector, θ_n and θ_a are the scaling exponents of the DFA analysis calculated with $Y(t')$ of healthy individuals and AD patients with closed eyes respectively. In the right sector, θ_n and θ_a are calculated with $|dY(t')|$ with open eyes

	$Y(t')$			$ dY(t') $		
	$\theta_n + 1$	With closed eyes		θ_n	With open eyes	
		$\theta_a + 1$	$\theta_a - \theta_n$		θ_a	$\theta_a - \theta_n$
$o1$	1.112(23)	1.188(43)	0.076	0.739(3)	0.756(12)	0.017
$o2$	1.069(21)	1.200(45)	0.131	0.758(3)	0.765(16)	0.070
$p3$	1.102(15)	1.165(33)	0.063	0.706(5)	0.746(11)	0.040
$p4$	1.132(29)	1.272(59)	0.140	0.722(5)	0.750(4)	0.028
$c3$	1.149(16)	1.219(28)	0.070	0.683(7)	0.745(15)	0.062
$c4$	1.144(14)	1.224(34)	0.080	0.729(6)	0.760(7)	0.031
$t3$	1.181(33)	1.283(45)	0.102	0.722(25)	0.766(19)	0.044
$t4$	1.188(22)	1.213(27)	0.025	0.770(22)	0.770(15)	0.000
$f3$	1.188(16)	1.261(27)	0.073	0.693(6)	0.720(9)	0.027
$f4$	1.202(18)	1.255(32)	0.053	0.650(10)	0.755(8)	0.105

healthy individuals and θ_a for AD patients take the values smaller than 0.5. Therefore, EEG dynamics is long-range anti-correlated in time. In addition, both θ_n and θ_a show an increasing trend from the o channels to f channels.

For every channel, $\theta_a - \theta_n$ is positive. This indicates that the AD disease *does* change the interactions among the neural cells, and therefore the dynamic scaling behavior. Essentially, a bigger θ_a represents a slower dynamics of the AD patients. This is consistent with the finding in the preceding section. From the microscopic viewpoint, the slower dynamics should originate from the partial breaking down of the interactions among the neural cells.

To investigate how the α peak affects the dynamic behavior, one may calculate the DFA functions with $Y_c(t')$. For $F(t)$ of $Y_c(t')$, the ‘oscillation’ around $t = 25$ becomes almost invisible. In later times, the curves of $Y(t')$ and $Y_c(t')$ yield similar values of the exponent $\theta + 1$. Therefore, we conclude that for the DFA analysis, the α peak only perturbs the dynamic behavior at early times.

The application of the DFA analysis to $dY(t')$ should yield $F(t) \sim t^\theta$. Our calculations indeed confirm this, and it is shown in Fig. 5(a). Since the exponent θ is small, the power-law behavior looks slightly less clean. Nevertheless, the exponent θ estimated here is in consistence with that given in Table 1.

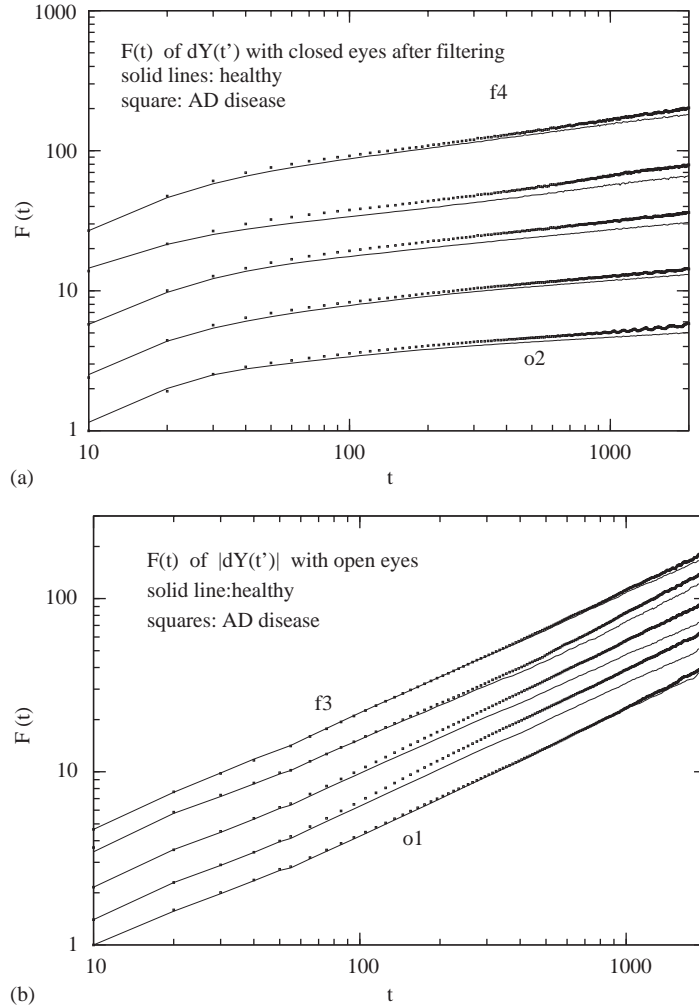


Fig. 5. (a) DFA functions of $dY(t')$ of the $o2$, $p4$, $c4$, $t4$ and $f4$ channels (from below) with closed eyes after filtering out the α peaks are plotted in log–log scale. Solid lines and square lines are for healthy individuals and AD patients, respectively. (b) DFA functions of $|dY(t')|$ of the $o1$, $p3$, $c3$, $t3$ and $f3$ channels (from below) with open eyes before filtering out the α peaks. Solid lines and square lines are for healthy individuals and AD patients, respectively.

Since $dY(t')$ is anti-correlated in time, it is not very convenient to directly measure the auto-correlation function. The DFA method is an efficient approach to this kind of dynamics. To understand the dynamic behavior of $dY(t')$, it is suggested in Refs. [4] that $dY(t')$ may be decomposed into two time series $|dY(t')|$ and $Sgn(dY(t'))$. $Sgn(dY(t'))$ remains anti-correlated in time, while $|dY(t')|$ is long-range correlated in time, as demonstrated in the previous section. In Fig. 5(b), $F(t)$ calculated from $|dY(t')|$ of the EEG with open eyes is plotted on a log–log scale. The power-law behavior is clearly seen. In Table 1, the values of the exponent θ measured from figures like Fig. 5(b) show a decreasing trend from o channels to f channels. The value $1.0 > \theta > 0.5$ indicates that the time series of $|dY(t')|$ is long-range correlated in time. Similar as in the case of $Y(t')$, different values of the exponent θ for healthy individuals and AD patients are also detected, but the difference is less prominent.

To summarize, the DFA analysis reveals that the time series of $|dY(t')|$ is long-range correlated in time, while $dY(t')$ and $Sgn(dY(t'))$ are temporally anti-correlated. The scaling exponent θ of the AD patients takes values different from those of the healthy individuals. The difference is less prominent for the EEG with open eyes, possibly due to noises from the environment.

5. Conclusions

In conclusion, we have investigated the dynamic scaling behavior of the human brain EEG with both open and closed eyes, and for both healthy individuals and AD patients. (i) The probability distribution $P(\Delta Y_c, \Delta t)$ obeys a dynamic scaling form. The calculations of the auto-correlation functions and persistence probabilities, together with the DFA analysis, reveal that the time series $|dY(t')|$ is long-range correlated in time, while $dY(t')$ and $Sgn(dY(t'))$ are temporally anti-correlated. (ii) A filtering technique is introduced to study the effect of the α and β oscillations. It is observed that this technique is important in revealing the dynamic scaling form of $P(\Delta Y_c, \Delta t)$, while it does not affect so much the dynamic behavior of some other observables. (iii) Our calculations show that the dynamics of the EEG of the AD patients is somewhat slower than that of the healthy individuals.

In a very recent work [25], functional networks connecting correlated human brain sites are extracted from functional magnetic resonance imaging. Analysis shows that the resulting networks are scale free with small-world properties. Our results presented in this paper and in Ref. [16] are in agreement with such a view to the human brain. Possibly, models based on complex networks may be constructed for understanding the dynamics of the human brain EEG.

Acknowledgements

Work supported in part by DFG (Germany) under Grant No. TR 300/3-3, NNSF (China) under Grant Nos. 10325520 and 70371069. The authors deeply thank Q.Y. Tong for the experimental data.

References

- [1] B. Bak, C. Tang, K. Wiesenfeld, Phys. Rev. Lett. 59 (1987) 381.
- [2] V. Frete, K. Christensen, A.M. Sorensen, J. Feder, T. Jossang, P. Meakin, Nature 379 (1996) 49.
- [3] K. Linkenkaer-Hansen, V.V. Nikouline, J.M. Palva, R.J. Ilmoniemi, J. Neurosci. 21 (2001) 1370.
- [4] Y. Ashkenazy, P.Ch. Ivanov, S. Havlin, C.K. Peng, A.L. Goldberger, H.E. Stanley, Phys. Rev. Lett. 86 (2001) 1900.
- [5] V. Schulte-Frohlinde, Y. Ashkenazy, P.Ch. Ivanov, L. Glass, A.L. Goldberger, H.E. Stanley, Phys. Rev. Lett. 87 (2001) 068104.
- [6] K. Koscielny-Bunde, A. Bunde, S. Havlin, H.E. Roman, Y. Goldreich, H.J. Schellnhuber, Phys. Rev. Lett. 81 (1998) 729.
- [7] R.N. Mantegna, H.E. Stanley, Nature 376 (1995) 46.
- [8] V.M. Eguiluz, M.G. Zimmermann, Phys. Rev. Lett. 85 (2000) 5659.
- [9] P. Jefferies, M.L. Hart, P.M. Hui, N.F. Johnson, Int. J. Theory Appl. Finance 3 (2000) 3.
- [10] V. Plerou, P. Gopikrishnan, H.E. Stanley, Nature 421 (2003) 130.
- [11] B. Zheng, F. Ren, S. Trimper, D.F. Zheng, Physica A 343 (2004) 653.
- [12] B. Zheng, T. Qiu, F. Ren, Phys. Rev. E 69 (2004) 046115.
- [13] C.K. Peng, S. Havlin, H.E. Stanley, A.L. Goldberger, Chaos 5 (1995) 82.
- [14] N. Sapir, R. Karasik, S. Havlin, et al., Phys. Rev. E 67 (2003) 031903.
- [15] P. Gong, A.R. Nikolaev, C. van Leeuwen, Neurosci. Lett. 336 (2003) 33.
- [16] C.P. Pan, B. Zheng, Y.Z. Wu, Y. Wang, X.W. Tang, Phys. Lett. A 329 (2004) 130.
- [17] C. Besthorn, H. Förstl, C. Geiger-Kabisch, H. Sattel, T. Gasser, U. Schreiter-Gasser, Electroen. Clin. Neurophysiol. 90 (1994) 242.
- [18] S.N. Majumdar, A.J. Bray, S. Cornell, C. Sire, Phys. Rev. Lett. 77 (1996) 3704.
- [19] K. Oerding, F. van Wijland, J. Phys. A 31 (1998) 7011.
- [20] B. Zheng, Int. J. Mod. Phys. B 12 (1998) 1419 review article.
- [21] F. Ren, B. Zheng, Phys. Lett. A 313 (2003) 312.
- [22] C.K. Peng, S.V. Buldyrev, S. Havlin, M. Simons, H.E. Stanley, A.L. Goldberger, Phys. Rev. E 49 (1994) 1685.
- [23] J.W. Kantelhardt, S. Zschiegner, E. Koscielny-Bunde, S. Havlin, A. Bunde, H.E. Stanley, Physica A 316 (2002) 87.
- [24] A. Carbone, G. Castellì, H.E. Stanley, Physica A 344 (2004) 267.
- [25] V.M. Eguiluz, D.R. Chialvo, G.A. Cecchi, M. Baliki, A.V. Apkarian, Phys. Rev. Lett. 94 (2005) 018102.